Supporting Information

Improved Electrochemical Reduction of CO_2 to Syngas with Highly Exfoliated $Ti_3C_2T_x$ MXene-Gold Composite

Murugan Krishnan, [a] Aathilingam Vijayaprabhakaran, [a][b] Murugavel Kathiresan, [a]*

[a] Electro Organic & Materials Electrochemistry Division

CSIR-Central Electrochemical Research Institute, Karaikudi – 630003, Tamil Nadu, India.

[b] Academy of Scientific and Innovative Research (AcSIR), Ghaziabad- 201002, India.

E-mail: kathiresan@cecri.res.in

Experimental Section

Synthesis of $Ti_3C_2T_x$ thin sheets

$Ti_3C_2T_x$ thin sheets were prepared by minimally intensive layer delamination (MILD) method. Briefly, 1.0 g of Ti_3AlC_2 was introduced to a solution made of 1.6 mL 48 wt % HF (Sigma-Aldrich), 7 mL of 37 wt % HCl (Sigma-Aldrich), and 11.4 mL of deionized water (DI). A loosely capped high density polyethylene bottle was used as the etching container. The prepared solution was stirred with 500 rpm for 24 h at 35 °C. The etched Al−Ti_3C_2 was washed with DI water via repeated centrifugation and decantation cycles until the supernatant reached pH ~ 6 using a centrifuge tube. Once the $Ti_3C_2T_x$ was neutralized, the washing process was complete. The etched multilayer $Ti_3C_2T_x$ sediment was then dispersed in a 0.5 M solution of LiCl used to start the delamination process. The $Ti_3C_2T_x$/LiCl suspension was then stirred at 400 rpm for a minimum of 4 h at room temperature. The $Ti_3C_2T_x$/LiCl suspension was then washed with DI water via repeated centrifugation and decantation of the supernatant using a centrifuge tube. Next, the residue was dispersed by ultrasonication, exfoliation was carried out to separate the layers of $Ti_3C_2T_x$ into 2D sheets for 4 h under nitrogen. The suspension was centrifuged for 10 min with 3500 rpm to remove the unexfoliated $Ti_3C_2T_x$. Finally, the $Ti_3C_2T_x$ thin sheets were obtained by filtration and dried in vacuum for further experiment.[1]

Synthesis of Au/$Ti_3C_2T_x$

To create Au/$Ti_3C_2T_x$ nanocomposites, the $HAuCl_4$ crystals (1 wt%) were dissolved in deionized water and subsequently mixed with the dispersion of $Ti_3C_2T_x$ (1 mg.mL^{-1}) in a beaker. The redox reaction between $HAuCl_4$ and $Ti_3C_2T_x$ was carried out at 40°C for 30 minutes to synthesize Au/$Ti_3C_2T_x$ nanocomposites. After the reaction, the composites were centrifuged and then dispersed in an isopropanol solution prior to use.

The flowchart depicted in **Figure 1** illustrates the preparation procedure for the Au/$Ti_3C_2T_x$ nanocomposites. The reaction between MXene materials and Au^{3+} can be represented by the following equation:

$$Ti_3C_2F_x(OH)_y + 3\delta e^- + \delta Au^{3+} \rightarrow Ti_3C_2F_x(OH)_y + \delta Au^0 \qquad (1)$$

Equation (1) describes the reaction involving $Ti_3C_2F_x(OH)_y$, which represents Ti_3C_2 (MXene) materials with surface -F and -OH groups. $HAuCl_4$ crystals dissolved to form Au^{3+} in solution. MXenes terminated with -OH groups can facilitate the reduction of noble metal ions to zero-

valent metals.[2] Throughout the reaction, certain amounts of Au^{3+} ions were reduced to gold nanoparticles, which were then deposited onto the Ti_3C_2 (MXene) materials upon interaction with $Ti_3C_2F_x(OH)_y$.

Contact angle measurements

To conduct contact angle measurements, a 5 µL droplet of deionized (DI) water was applied onto the $Au/Ti_3C_2T_x$-coated surface of the carbon cloth. A camera equipped with a macro lens captured the contact angles. The contact angle images were processed using ImageJ software.

Electrochemical characterization

Electrochemical measurements were performed in a three-electrode electrochemical cell connected to an electrochemical workstation (Autolab) carbon cloth decorated with $Au/Ti_3C_2T_x$ was used as the working electrode (1 cm^2), a platinum foil as the counter electrode, and Ag/AgCl (saturated KCl) as the reference electrode. The electrode potentials are converted to the RHE according to the equation $E_{(RHE)} = E(Ag/AgCl) + 0.059\ pH + 0.210\ V$. The cathode and anode chambers were separated by a proton exchange membrane (Nafion 117). Each chamber was filled with 20 ml of 0.1 M $KHCO_3$ solution. CO_2 (99.995%) was purged at a flow rate of 20 sccm into the cathode chamber for 30 min before each ECRR measurement with continued purging throughout the measurement. The solution pH after purging with CO_2 was 6.7. The proposed electrochemical cell setup for the ECRR is shown in below.

The catalytic activity of $Au/Ti_3C_2T_x$ catalysts was measured in a range of potentials from 0.2 to -2.0 V *vs*. Ag/AgCl. All electrochemical measurements were performed at 25 °C and atmospheric pressure employing an AutoLab double channel potentiostat with a built-in impedance spectrometer. The current density normalized by the electrochemical active surface area (ECSA) for the as-prepared catalysts was computed through,

$$\text{ECSA-normalized current density} = \text{current density} \times C_{dl}/C_s$$

Product analysis

During chronoamperometry, gaseous products were analysed using in situ using gas chromatography, and liquid products were analyzed from quantitative nuclear magnetic resonance (qNMR) spectroscopy using dimethyl sulfoxide as an internal standard. Solvent presaturation technique was implemented to suppress the water peak. Faradaic efficiencies

were calculated from the amount of charge passed to produce each product, divided by the total charge passed at a specific time or during the overall run.

Gas production was measured on an Agilent gas chromatography instrument (model #8890 customised) equipped with a Haysep D column (1/8" × 6') and a 13 × Mol Sieve column (1/8" × 6'); carbon monoxide (CO) was quantified using flame ionization detector (FID) and hydrogen (H_2) using thermal conductivity detector (TCD). All potentials in this study were measured against the RHE reference electrode After the electrochemical cell was assembled, the electrolyte solution in the working compartment was sparged for 30 minutes with CO_2. The solutions were electrolyzed at a constant potential for a desired test period. After electrolysis, the headspace of the cell was analyzed by GC. The 0.1 M $KHCO_3$ solution after electrolysis was collected and analyzed on a Bruker 500 MHz NMR spectrometer to quantify liquid products. Samples of the $KHCO_3$ solution after electrolysis were analyzed by quantitative ^1H NMR using dimethyl sulfoxide as an internal standard. For NMR measurements, 0.5 ml of electrolyte solution was mixed with 0.1 ml deuterium oxide (D_2O, 99.9%) and dimethyl sulfoxide (DMSO, 7 mM) was added as an internal standard. The ^1H spectrum was measured with water suppression by a pre-saturation method.

The FE values for products were calculated using the following equation:

$$\%FE_{\text{products}} = \frac{n\ F\ mol}{Q} \times 100$$

where n, mol, F, and Q are the number of electrons, number of moles of products, Faraday's constant (96485 C mol^{-1}), and total charges passed, respectively.

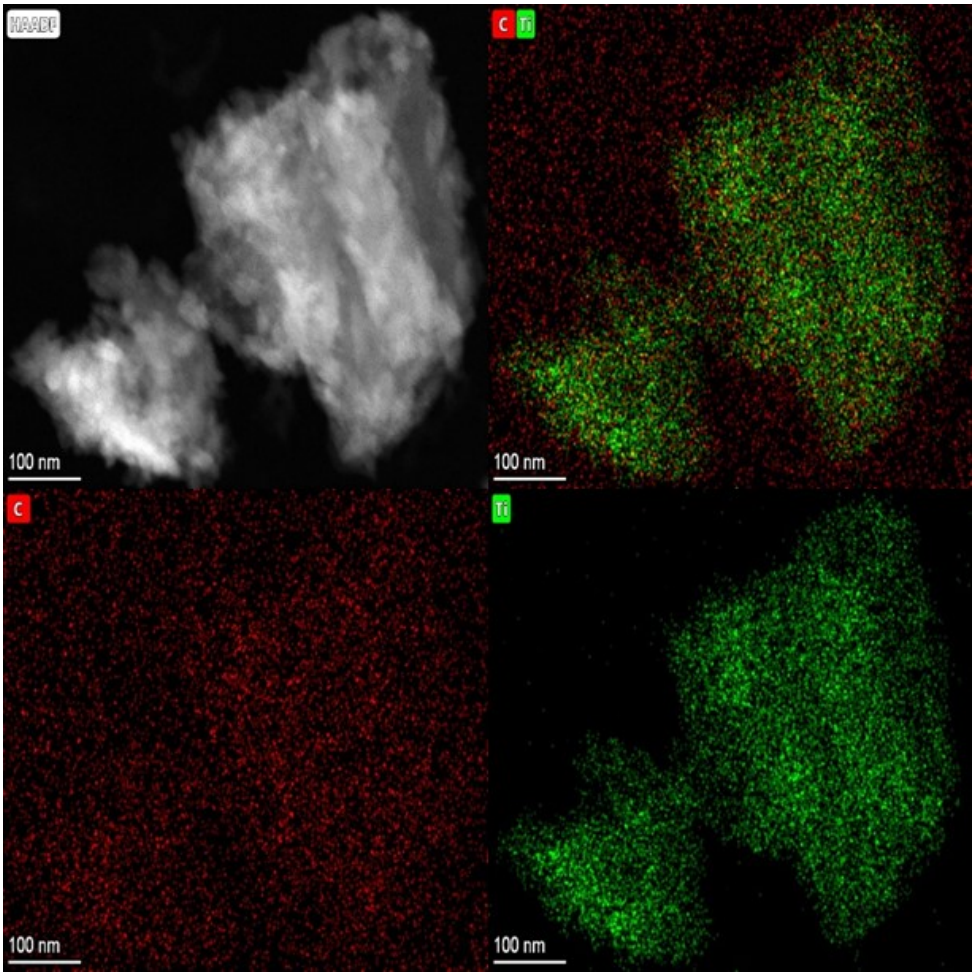

Fig. S1. HAADF-TEM images of $Ti_3C_2T_x$

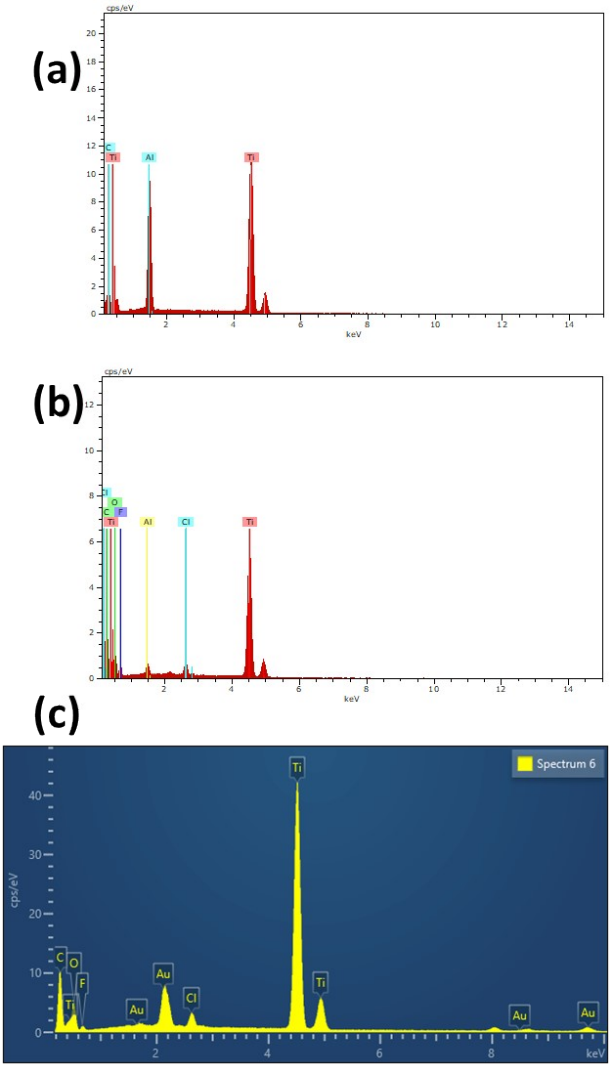

Materials	Elements	Weight %
Ti_3AlC_2	Ti	68.48
	Al	15.67
	C	15.86

Materials	Elements	Weight %
$Ti_3C_2T_x$	Ti	50.92
	Al	0.93
	C	20.44
	O	18.75
	F	7.48
	Cl	1.47

Materials	Elements	Weight %
$Au/Ti_3C_2T_x$	Au	8.93
	Ti	40.52
	C	23.56
	O	22.42
	F	3.36
	Cl	1.20

Fig. S2. EDS images of (a) Ti_3AlC_2, (b) $Ti_3C_2T_x$ and (c) $Au/Ti_3C_2T_x$

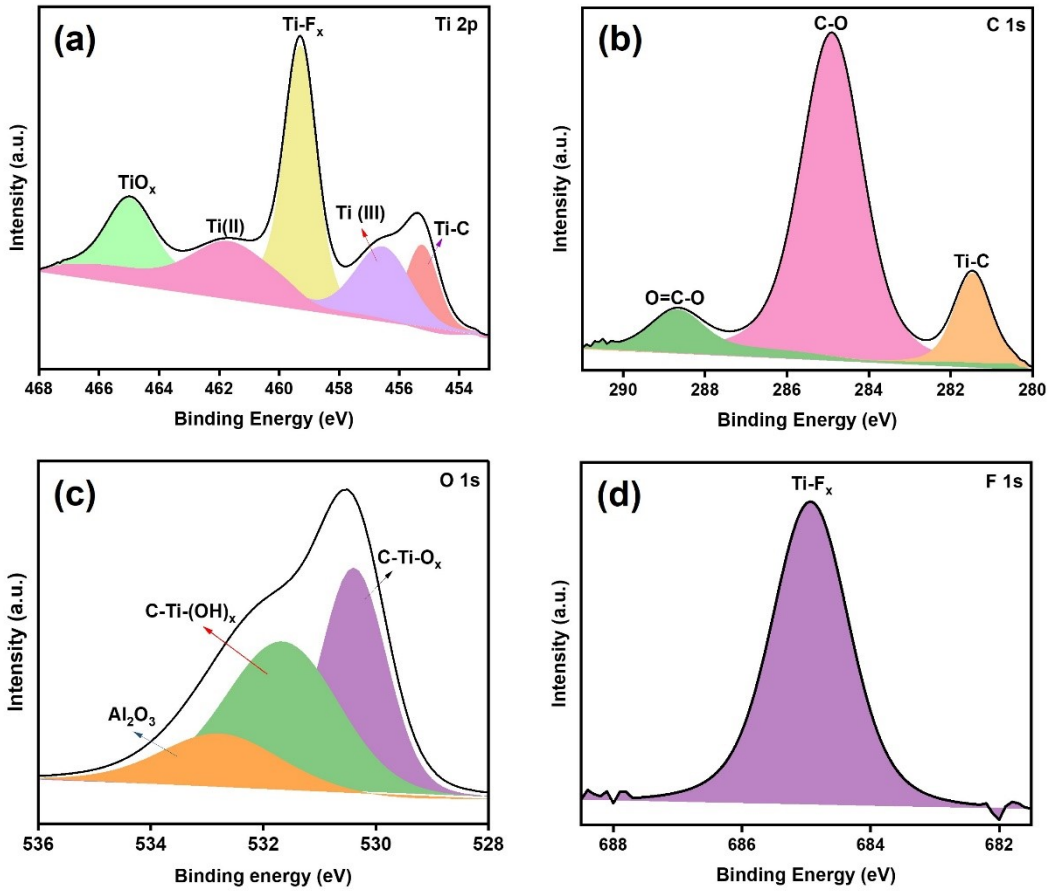

Fig. S3. The XPS spectra of (a) Ti 2p, (b) C 1s, (c) O 1s and (d) F 1s of $Ti_3C_2T_x$.

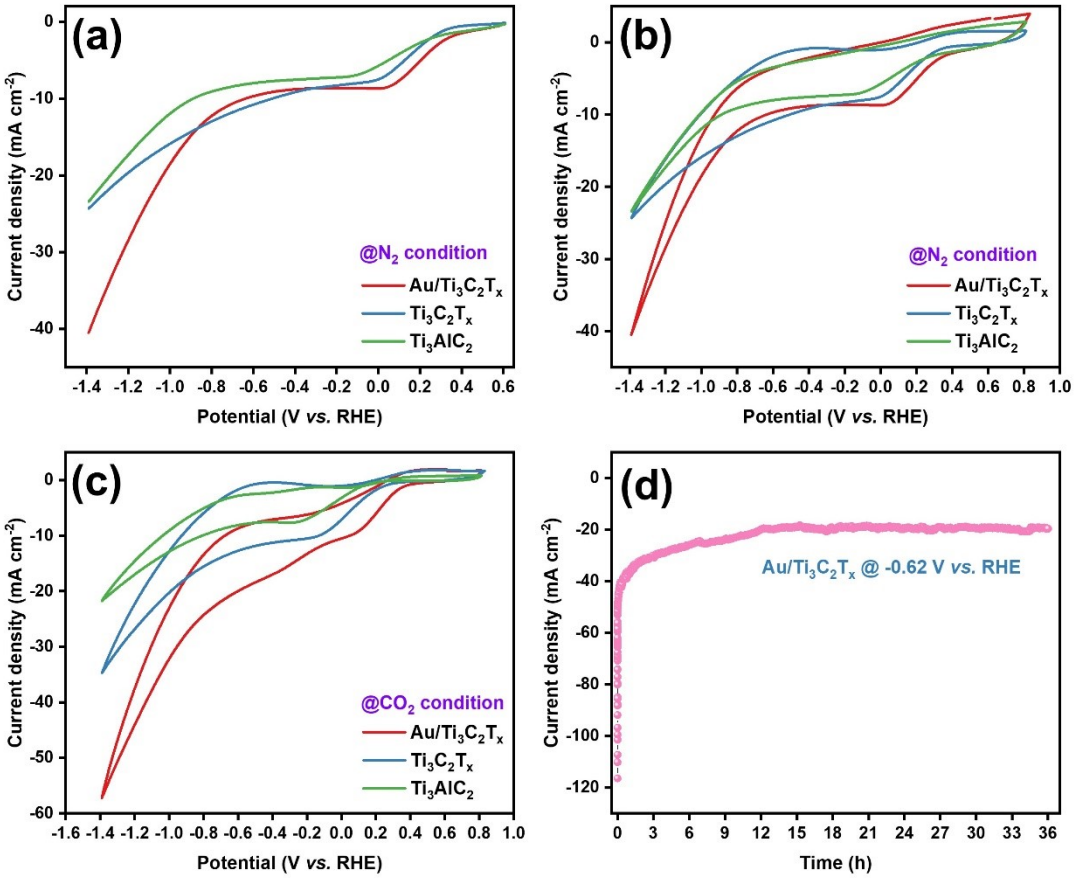

Fig. S4. (a) LSVs, (b) CVs in a N_2-saturated 0.1 M $KHCO_3$ solution (c) CVs measured in CO_2 saturated 0.1 M $KHCO_3$ at room temperature, (d) Long-term chronoamperometry in CO_2 saturated 0.1 M $KHCO_3$.

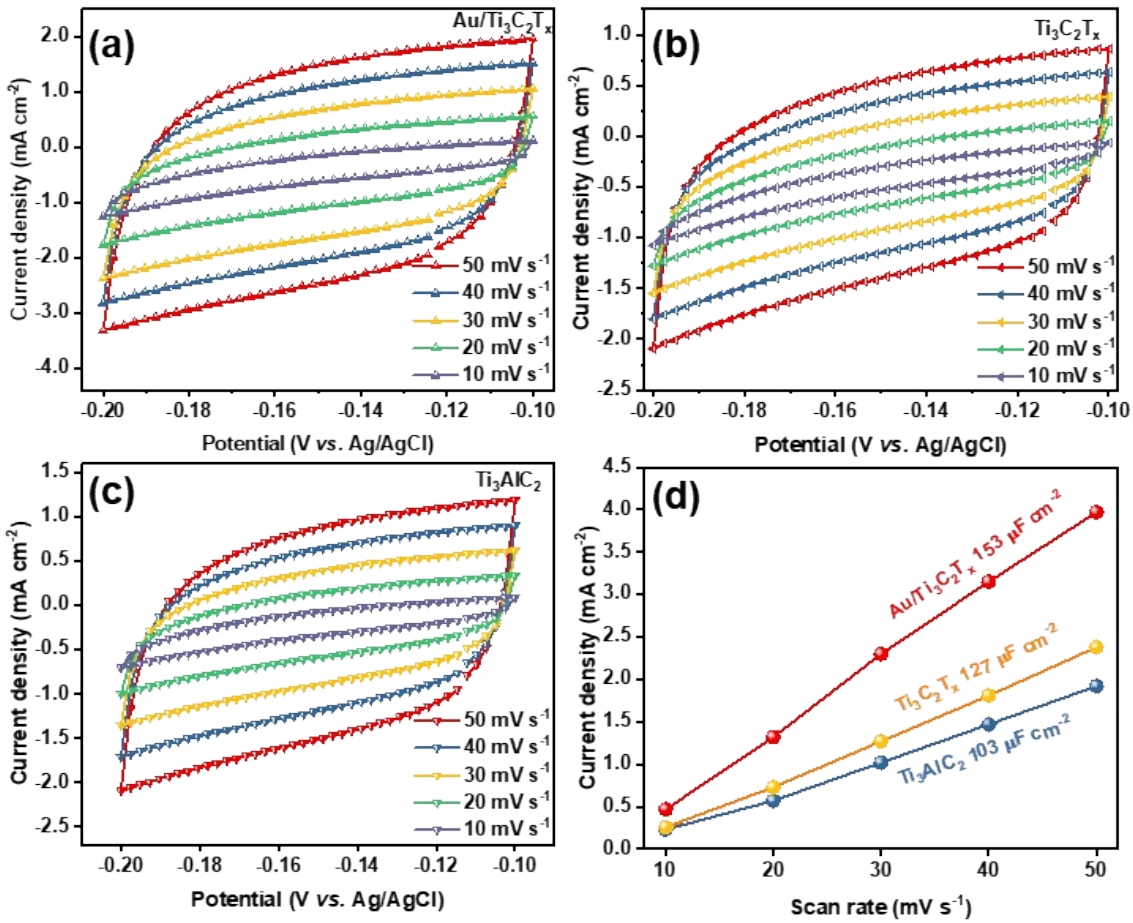

Fig. S5. (a) CV curves of (a) $Au/Ti_3C_2T_x$, (b) $Ti_3C_2T_x$, (c) Ti_3AlC_2 at the scan rate of 10, 20, 30, 40, 50 mV s^{-1} (d) Electrochemical double layer plot.

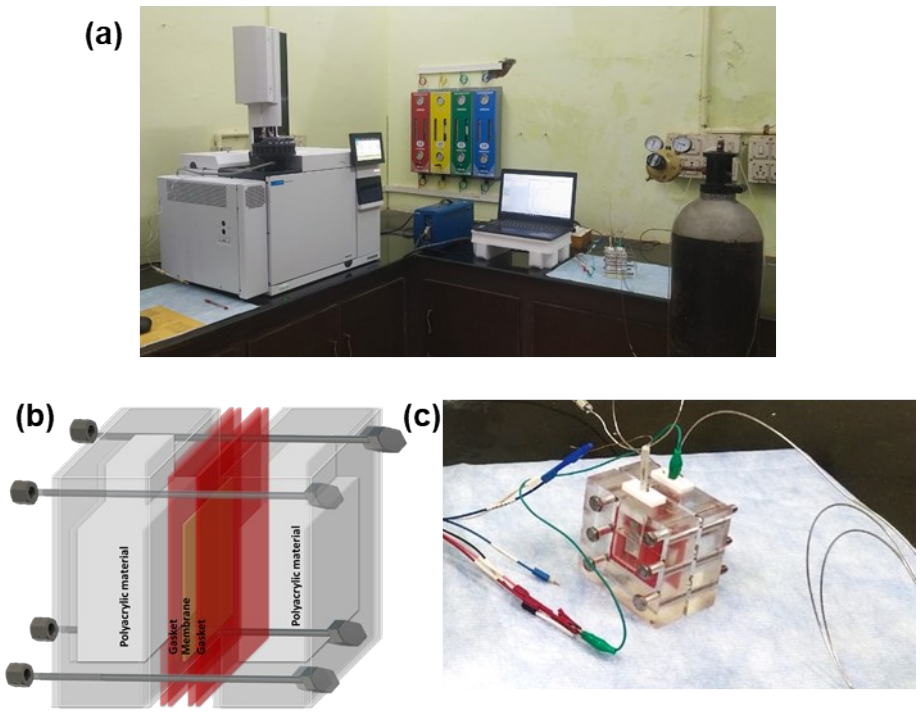

Fig. S6. (a) Electrochemical workstation (b) schematic Cell design (c) Experimental cell setup

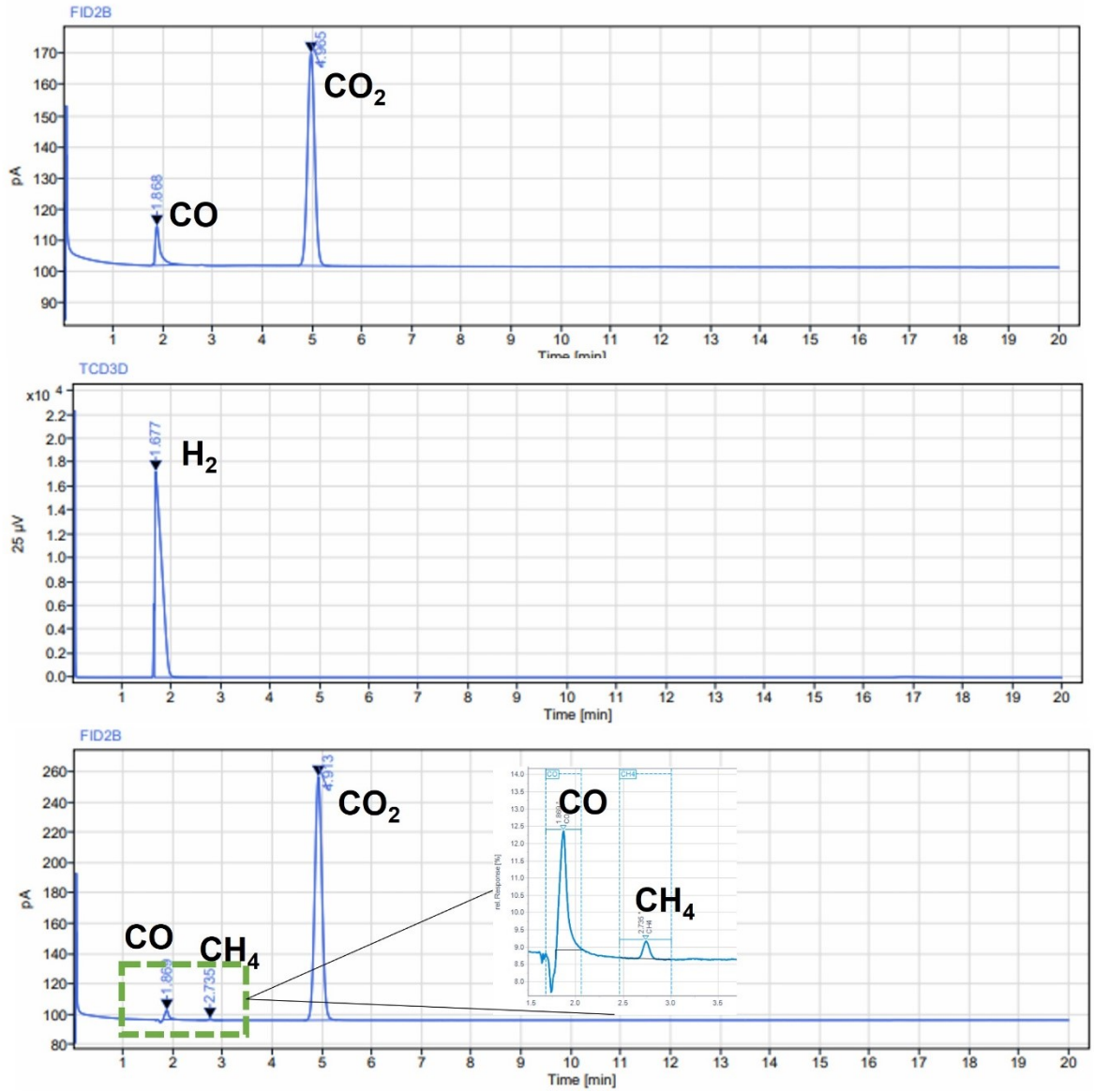

Fig. S7. GC traces from FID and TCD channels. Peaks corresponding to the observed gaseous products are indicated.

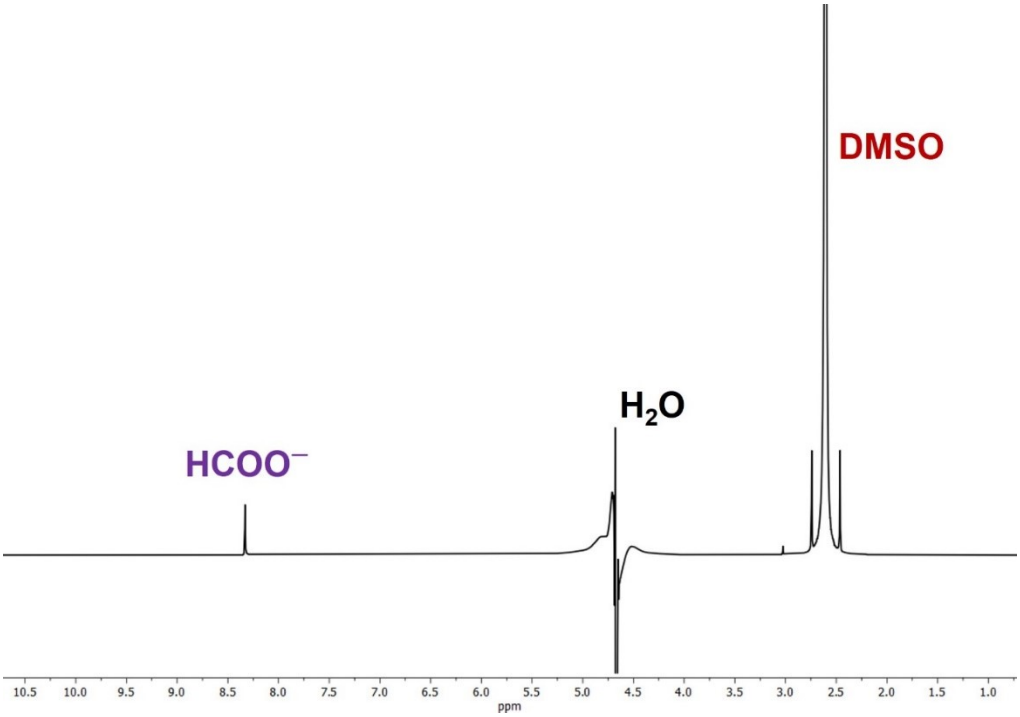

Fig. S8. A representative ^{1}H NMR spectrum collected from the liquid product

Catalyst	Electrolyte	Product	FE (%)	Current density (mA/cm^2)	Potential	Reference
Au_n/C-paper	0.2 M $KHCO_3$	CO, H_2	89	-4.0	−1.5 V *vs.* Ag/AgCl	[3]
Au-CeO_2-DP	0.1 M $KHCO_3$	CO	95	NA	−0.7 V *vs.* RHE	[4]
20%Au/FPC-800	0.1 M $KHCO_3$	CO	92	10.5	−0.7 V *vs.* RHE	[5]
M-AuPd(20)	0.1 M $KHCO_3$	HCOOH	99	6.5 → 5.2	−0.25 V *vs.* RHE	[6]
AgAu nanomesh	0.1 M $KHCO_3$	CO	99	NA	− 0.90 V *vs.* RHE	[7]
$AuCu_3$@Au	0.5 M $KHCO_3$	CO	97.3	5.3	−0.6 V *vs.* RHE	[8]
ZnO-Fe-$Ti_3C_2T_x$	0.5 M NaOH	HCOOH	NA	18.745	−0.7 V *vs.* Ag/AgCl	[9]
Cu/$Ti_3C_2T_x$	0.1 M $NaHCO_3$	HCOOH CH_3OH	58.1	-1.08	−1.5 V *vs.* Ag/AgCl	[10]
Pd/$Ti_3C_2T_x$	1.0 M $KHCO_3$	CH_3OH	67.8	−4.1	−0.5 V *vs.* RHE	[11]
Au/$Ti_3C_2T_x$	0.1 M $KHCO_3$	CO H_2	48.3 25.6	-17.3 -25.6	−0.42 V *vs.* RHE	This work

Table S1. Comparison of Au and other MXene based electrocatalyst for CO_2 reduction

References

1. O. Salim, K. A. Mahmoud, K. K. Pant and R. K. Joshi, *Mater. Today Chem.*, 2019, **14**, 100191.
2. R. Cheng, T. Hu, M. Hu, C. Li, Y. Liang, Z. Wang, H. Zhang, M. Li, H. Wang, H. Lu, Y. Fu, H. Zhang, Q.-H. Yang and X. Wang, *J. Mater. Sci. Technol.*, 2020, **40**, 119-127.
3. S. K. Sharma, H. T. Ahangari, B. Johannessen, V. B. Golovko and A. T. Marshall, *Electrocatalysis*, 2023, **14**, 611-623.
4. X.-C. Sun, K. Yuan, J.-H. Zhou, C.-Y. Yuan, H.-C. Liu and Y.-W. Zhang, *ACS Catalysis*, 2022, **12**, 923-934.
5. Y. Cui, Y. Cheng, C. Yang, Y. Su, D. Yao, B. Liufu, J. Li, Y. Fang, S. Liu, Z. Zhong, X. Wang, Y. Song and Z. Li, *ACS Sustainable Chem. Eng.*, 2023, **11**, 11229-11238.
6. J. Bok, S. Y. Lee, B.-H. Lee, C. Kim, D. L. T. Nguyen, J. W. Kim, E. Jung, C. W. Lee, Y. Jung, H. S. Lee, J. Kim, K. Lee, W. Ko, Y. S. Kim, S.-P. Cho, J. S. Yoo, T. Hyeon and Y. J. Hwang, *J. Am. Chem. Soc.*, 2021, **143**, 5386-5395.
7. J.-L. Sang, L. Yu, X.-W. Song, W.-C. Geng, Y. Zhang and Y.-J. Li, *J. Alloys Compd.*, 2023, **944**, 169155.
8. X. Ma, Y. Shen, S. Yao, C. An, W. Zhang, J. Zhu, R. Si, C. Guo and C. An, *J. Mater. Chem. A*, 2020, **8**, 3344-3350.
9. K. Kannan, M. H. Sliem, A. M. Abdullah, K. K. Sadasivuni and B. Kumar, *Catalysts*, 2020, **10**, 549.
10. K. Eid, Q. Lu, S. Abdel-Azeim, A. Soliman, A. M. Abdullah, A. M. Abdelgwad, R. P. Forbes, K. I. Ozoemena, R. S. Varma and M. F. Shibl, *J. Mater. Chem. A*, 2022, **10**, 1965-1975.
11. B. Govindan, R. Madhu, M. Abu Haija, F. V. Kusmartsev and F. Banat, *Catalysts*, 2022, **12**, 1180.